Glucagon-Like Peptide-1 Receptor PET/CT with ^{68}Ga-NOTA-Exendin-4 for Detecting Localized Insulinoma: A Prospective Cohort Study

Yaping Luo[1], **Qingqing Pan**[1], **Shaobo Yao**[1], **Miao Yu**[2], **Wenming Wu**[3], **Huadan Xue**[4], **Dale O. Kiesewetter**[5], **Zhaohui Zhu**[1], **Fang Li**[1], **Yupei Zhao**[3], and **Xiaoyuan Chen**[5]

[1]Department of Nuclear Medicine, Chinese Academy of Medical Sciences and Peking Union Medical College Hospital, Beijing, China [2]Department of Endocrinology, Chinese Academy of Medical Sciences and Peking Union Medical College Hospital, Beijing, China [3]Department of General Surgery, Chinese Academy of Medical Sciences and Peking Union Medical College Hospital, Beijing, China [4]Department of Radiology, Chinese Academy of Medical Sciences and Peking Union Medical College Hospital, Beijing, China [5]Laboratory of Molecular Imaging and Nanomedicine, National Institute of Biomedical Imaging and Bioengineering, National Institutes of Health, Bethesda, Maryland

Abstract

Preoperative localization of insulinoma is a clinical dilemma. We aimed to investigate whether glucagon-like peptide-1 receptor (GLP-1R) PET/CT with ^{68}Ga-NOTA-MAL-cys^{40}-exendin-4 (^{68}Ga-NOTA-exendin-4) is efficient in detecting insulinoma.

Methods—In our prospective cohort study, patients with endogenous hyperinsulinemic hypoglycemia were enrolled. CT, MRI, endoscopic ultrasound, and ^{99m}Tc-hydrazinonicotinamide-TOC SPECT/CT were done according to standard protocols. GLP-1R PET/CT was performed 30–60 min after the injection of ^{68}Ga-NOTA-exendin-4. The gold standard for diagnosis was the histopathologic results after surgery.

Results—Of 52 recruited patients, 43 patients with histopathologically proven insulinomas were included for the imaging studies. Nine patients did not undergo surgical intervention. ^{68}Ga-NOTA-exendin-4 PET/CT correctly detected insulinomas in 42 of 43 patients with high tumor uptake (mean $SUV_{avg} \pm SD$, 10.2 ± 4.9; mean $SUV_{max} \pm SD$, 23.6 ± 11.7), resulting in sensitivity of 97.7%. In contrast, ^{99m}Tc-hydrazinonicotinamide-TOC SPECT/CT showed a low sensitivity of 19.5% (8/41) in this group of patients; however, it successfully localized the tumor that was false-negative with GLP-1R PET/CT. The sensitivities of CT, MR, and endoscopic ultrasonography were 74.4% (32/43), 56.0% (14/25), and 84.0% (21/25), respectively.

For correspondence or reprints contact either of the following: Yupei Zhao, Department of Nuclear Medicine, Chinese Academy of Medical Sciences and Peking Union Medical College Hospital, Beijing, China 100730. zhaoyp_pumch@163.com, Xiaoyuan Chen, Laboratory of Molecular Imaging and Nanomedicine, National Institute of Biomedical Imaging and Bioengineering, National Institutes of Health, Bethesda, MD 20892. shawn.chen@nih.gov.

Conclusion—^{68}Ga-NOTA-exendin-4 PET/CT is a highly sensitive imaging technique for the localization of insulinoma.

Keywords

glucagon-like peptide-1 receptor (GLP-1R); exendin-4; PET/CT; insulinoma

---

Insulinoma is the most common cause of endogenous hyperinsulinemic hypoglycemia in adult patients without diabetes. The diagnosis of insulinoma is based on demonstrating inappropriately high serum insulin concentrations during a spontaneous or induced episode of hypoglycemia. Imaging techniques are then used to localize the tumor, which is critical for diagnosis and surgical treatment. Conventional imaging procedures such as contrast-enhanced CT, MRI, and endoscopic ultrasonography (EUS) have limited accuracy in localizing insulinomas because of the small size of these tumors (1–4). The current gold standard, that is, intraoperative ultrasound with manual palpation, yields a sensitivity of only about 80% (5). Somatostatin receptor scintigraphy (SRS) is considered to be the most sensitive method for neuroendocrine tumors. In contrast to other neuroendocrine tumors, the sensitivity of SRS for insulinomas is low because of the low expression of somatostatin receptor subtype 2 (sstr2) in these tumors (6,7).

In recent years, a new receptor-targeted imaging technique, glucagon-like peptide-1 receptor (GLP-1R) imaging, for detecting insulinoma has been established. GLP-1R is expressed on benign insulinoma cell surfaces with very high incidence (>90%) and density (8,133 dpm/mg of tissue). No other peptide receptor has been found to exhibit such high expression levels in insulinoma (8,9). The first clinical study with GLP-1R imaging using [Lys^{40}(Ahx-DTPA-^{111}In)NH$_2$]-exendin-4 (DTPA is diethylenetriamine tetraacetic acid), which is a stable agonist of GLP-1R, was successfully performed on 2 patients with insulinoma (10). Subsequently, clinical studies with ^{111}In- and ^{99m}Tc-labeled exendin-4 showed high sensitivity for GLP-1R imaging in detecting insulinomas with SPECT (11–13). Because imaging modalities need to be highly sensitive on account of the small size of insulinoma, PET may offer an advantage over SPECT, with higher spatial resolution, sensitivity, and imaging contrast. So far, exendin-based PET tracers labeled with ^{68}Ga, ^{18}F, and ^{64}Cu have been successfully prepared (14–25). For ^{64}Cu, its long half-life (12.7 h) and β$^-$ emission can lead to an increased radiation burden for the patient. In a comparative study with ^{64}Cu- and ^{68}Ga-labeled exendin-4 peptides, the estimated mean effective dose for ^{64}Cu-labeled exendin-4 was 10-fold higher than that of the ^{68}Ga-labeled same ligand (24). ^{18}F is a favorable radionuclide for PET imaging, but except for a NOTA-conjugated exendin-4 probe (^{18}F-AlF-NOTA-MAL-cys^{40}-exendin-4) (19), most of the currently available ^{18}F-labeled exendin-based tracers show relatively high background uptake in the liver and intestines in xenograft models (15,18,20,22,23), which may partially limit clinical use. The tedious labeling procedure is another concern. For human use, ^{68}Ga is an excellent option because of its availability, low price, and short physical half-life. Recently, a pilot study revealed that ^{68}Ga-DOTA-exendin-4 PET/CT is a clinically feasible and sensitive tool for the detection of insulinomas (26). Our preliminary experience with ^{68}Ga-NOTA-MAL-cys^{40}-exendin-4 (^{68}Ga-NOTA-exendin-4) also showed that the tracer can localize occult insulinoma (27). The aim of this study was to examine the use of ^{68}Ga-NOTA-exendin-4

PET/CT in the detection of insulinomas and to compare its diagnostic value with that of conventional imaging.

MATERIALS AND METHODS

Study Design and Patients

In this prospective cohort study, we screened patients with hypoglycemia in the presence of neuroglycopenic symptoms and documented Whipple triad at the Peking Union Medical College Hospital (PUMCH). Patients were enrolled with the following inclusion criteria: biochemically proven endogenous hyperinsulinemic hypoglycemia (plasma glucose concentration < 3.0 mM, insulin > 3 μU/mL, and C-peptide > 0.6 ng/mL) and a negative screening for sulfonylurea and insulin autoantibody. We excluded patients with infantile-onset hypoglycemia, patients with renal insufficiency, and pregnant women. All patients eligible for the study were hospitalized and carefully examined for hypoglycemic etiologies (28). In addition to the conventional preoperative localization methods for insulinoma, patients were referred for ^{68}Ga-NOTA-exendin-4 PET/CT before elective surgery. All imaging procedures were performed within 1 mo of diagnosis. The presence of tumor was subsequently confirmed histopathologically, and the histologic type was determined. The study was approved by the institutional review board of PUMCH (protocol S-533) and registered at ClinicalTrials.gov (NCT 02560376). Written informed consent was obtained from each patient.

Preparation of ^{68}Ga-NOTA-MAL-Cys^{40}-Exendin-4

Synthesis of NOTA-MAL-cys^{40}-exendin-4 has been described previously (19). Radiolabeling with ^{68}Ga was performed manually immediately before injection. Briefly, 85 μL of sodium acetate (1.25 M) were added to 1 mL of ^{68}GaCl$_3$ eluent (370–555 MBq) obtained from a ^{68}Ge/^{68}Ga generator (Eckert & Ziegler) to adjust the pH to 3.5–4.0. After addition of an aliquot of 25–50 μL (1 μg/μl) of NOTA-MAL-cys^{40}-exendin-4, the mixture was heated to 100 °C for 15 min. The reaction solution was diluted to 5 mL and passed through a preconditioned Sep-Pak C18 Plus Light cartridge (Waters), which was eluted by 0.5 mL of 75% ethanol to obtain the final product. The radiochemical purity of the product was analyzed by radio–high-performance liquid chromatography (Supplemental Fig. 1 [supplemental materials are available at http://jnm.snmjournals.org]). The specific radioactivity was 23.7–55.9 GBq/μmol, and the radiochemical yield was around 60%–70% (not corrected for decay). ^{68}Ga-NOTA-exendin-4 injection was filtered through a 0.22-μm Millex-LG filter (EMD Millipore). The injectate was confirmed to be sterile and pyrogen-free before clinical use.

GLP-1R PET/CT

Patients fasted for at least 4 h to reduce endogenous secretion by the small intestines of GLP-1, which may compete with exendin-4 in binding with GLP-1R (29). A continuous infusion of glucose (10%) was administered to prevent hypoglycemic episodes during the fasting and PET/CT procedure. Blood glucose concentrations were monitored before injection of the radiopharmaceutical. ^{68}Ga-NOTA-exendin-4 (18.5–185 MBq, 7–25 μg) was intravenously injected over 2–3 min. Each patient was carefully checked for adverse events.

Torso PET/CT images (Biograph 64 TruePoint with TrueV option; Siemens) were acquired 30–60 min after injection (2–4 min/bed position), and late scans of the upper abdomen (5–7 min/bed position) were performed between 2 and 3 h after injection when necessary. All patients underwent unenhanced low-dose CT (120 kV, 30–50 mAs) for attenuation correction and anatomic reference. The acquired data were reconstructed using ordered-subset expectation maximization (2 iterations, 8 subsets, gaussian filter, 5 mm in full width at half maximum, 168×168 image size).

Conventional Imaging

Conventional imaging included contrast-enhanced CT, MRI, EUS, and SRS with ^{99m}Tc-hydrazinonicotinamide (HYNIC)-TOC. All imaging was performed at PUMCH except for MRI (detailed MRI protocols are listed in Supplemental Table 1). For contrast-enhanced CT (40 mL of iohexol [350 mg I/mL] and 50 mL of saline at 5 mL/s), a pancreatic perfusion scan (6-s delay, 25 dynamic datasets, 38.63-s total scanning time) was performed after a standard scan on a dual-source CT scanner (Somatom Definition Flash with Stellar Detector; Siemens) with the following parameters: 80 kV, 150 mAs, 0.28-s rotation time, 128×0.6 mm collimation, 3.0-mm reconstruction slice and increment, and B20f kernel. A curvilinear echoendoscope (EU-ME-1; Olympus) was used to perform EUS. For SRS, total-body planar images (16 cm/min) were acquired at 1 and 4 h after injection of ^{99m}Tc-HYNIC-TOC (555–740 MBq, 3–5 μg), and SPECT/CT scans (Precedence 16; GE Healthcare) were acquired at the 2- to 3-h time point (30 s/frame/6°, ×1 zoom).

Imaging Reporting and Statistical Analysis

All conventional scans were independently reported by experienced radiologists, endoscopic physicians, and nuclear medicine physicians. MR images from other centers were carefully interpreted and reported at PUMCH. Two experienced nuclear medicine physicians visually assessed GLP-1R scans and measured semiquantitative values on PET/CT.

Positive imaging that showed consistency between imaging, surgery, and histopathologic analysis was regarded as true-positive. In patient-based analysis, correct localization of at least one insulinoma with or without additional false-positive lesions detected by imaging was regarded as true-positive. False-negative imaging was defined as failure to correctly localize the insulinoma. The sensitivity and positive predictive value with 95% confidence interval were assessed in patient-based and lesion-based analyses. The McNemar test was used to statistically compare the sensitivity of GLP-1R PET/CT with each type of conventional imaging. For comparison of positive predictive values, we applied the generalized score statistics. All analyses were done with R, version 3.2.2.

RESULTS

Clinical Characteristics and Histology

We recruited 52 patients with biochemically proven endogenous hyperinsulinemic hypoglycemia from February 1, 2014, to July 31, 2015. The clinical characteristics and biochemical investigations are summarized in Table 1. There were 43 patients with histopathologically proven insulinomas, including 1 patient (patient 15) with malignant

insulinoma, and 2 patients (patients 16 and 33) with multiple endocrine neoplasia type 1. Forty-two patients with benign insulinoma (defined as absence of metastases) underwent surgical removal of 45 tumors (dimensions, 15.9 ± 10.5 mm; range, 7–68 mm) on the basis of preoperative imaging, and symptoms of hypoglycemia resolved immediately after surgery. Robot-assisted laparoscopic enucleation of insulinoma was performed on 31 patients. The patient with malignant insulinoma had distant metastasis to the liver and to the retroperitoneal and mediastinal lymph nodes, and liver biopsy was performed. Twenty-six patients had grade 1 insulinoma (World Health Organization grading system), and in 14 patients grade 2 tumors were identified. Histologic details were unavailable in 3 patients because the surgical procedure was not performed at our institute.

Nine patients did not undergo a surgical intervention. Three patients had positive GLP-1R imaging results that were highly suggestive of insulinoma, but they have declined surgery so far. The remaining 6 patients had negative results on GLP-1R imaging and on conventional imaging. Two patients (symptom onset at school age) had a confirmed activating glucokinase mutation of congenital hyperinsulinism. Two patients were clinically diagnosed as having nesidioblastosis—due to noninsulinoma pancreatogenous hypoglycemia syndrome in one and post–gastric bypass hypoglycemia in the other. A definite diagnosis could not be established in 2 patients.

Patients with a histologic diagnosis were included in the main assessments. Detailed information about the preoperative work-up with imaging and histopathology is presented in Table 2. Comparison of the sensitivity and positive predictive value of GLP-1R PET/CT and conventional imaging is listed in Table 3.

Conventional Imaging

Pancreatic perfusion scanning was done for all patients, and insulinoma was correctly diagnosed in 32 of 43 patients. In patient 22, with an insulinoma in the uncinate process of the pancreas, the tumor was diagnosed only retrospectively on CT after visualization of the lesion by GLP-1R imaging. CT images were also retrospectively reviewed after surgery in all 11 patients with false-negative CT scans, and all lesions were isoenhancing compared with the normal pancreas. MRI was performed on 25 patients, and tumors were not localized in 11 patients. Notably, in patient 42, except for the insulinoma in the body of the pancreas that was correctly localized on CT and MR, an additional lesion that was possibly an intrapancreatic accessory spleen in the tail of the pancreas was false-positive on both CT and MR. The patient recovered from hypoglycemia after enucleation of the tumor in the body of the pancreas.

Twenty-five patients underwent EUS, which correctly localized 22 lesions in 21 patients. EUS was performed after all other imaging modalities, including GLP-1R PET/CT. In patient 2, EUS was not able to detect the tumor in the tail of the pancreas; instead, a false-positive lesion in the head of the pancreas was seen. Intraoperative ultrasound and monitoring of serum glucose concentration excluded a preoperatively reported suggestive lesion. SRS was performed on 41 patients, and only 8 of 41 patients had positive results, including the patient with malignant insulinoma.

GLP-1R PET/CT

Because all patients received a continuous infusion of glucose, no episodes of severe hypoglycemia occurred. Five patients reported a transient palpitation at the time of injection that lasted a few seconds. Two patients experienced a short episode of vomiting, and 2 patients reported slight nausea after injection of the ^{68}Ga-NOTA-exendin-4. No other adverse effects were observed.

In patients with benign insulinoma, ^{68}Ga-NOTA-exendin-4 PET/CT correctly localized the tumor in 41 of 42 patients (44/45 tumors). The positive lesions exhibited intense radioactivity, and the average and maximum SUVs of the tumors were 10.2 ± 4.9 (range, 3.9–22.2) and 23.6 ± 11.7 (range, 6.4–57.5), respectively (for example, patients 33 and 42 in Figs. 1 and 2). The tumor-to-pancreas uptake ratio was 7.90 ± 4.14 (range, 3.8–24.0). No significant difference in SUVs or tumor-to-pancreas uptake ratios was observed between type G1 and G2 insulinomas.

The only false-negative case occurred for a type G2 insulinoma (patient 7), in a patient who presented with a 1-mo history of neuroglycopenia. CT and MR disclosed a 4.6×2.5 cm hyper-vascular tumor in the tail of the pancreas, suggestive of an insulinoma. ^{68}Ga-NOTA-exendin-4 PET/CT showed the tumor to be photopenic; meanwhile, intense radioactivity was visualized in the tumor on ^{99m}Tc-HYNIC-TOC SPECT/CT. The patient then underwent ^{18}F-FDG PET/CT to evaluate for malignancy. The tumor was ^{18}F-FDG–avid, and the SUV_{max} was 2.6.

In patient 15, with distant metastases, type G1 insulinoma was identified with liver biopsy. All the lesions seen on GLP-1R imaging (hot spots in the body of the pancreas, the liver, and the retroperitoneal and mediastinal lymph nodes) were also positive on ^{99m}Tc-HYNIC-TOC SPECT/CT, suggesting concomitant GLP-1R and sstr2 expression. The patient was then treated with octreotide.

Late scanning was performed 2–3 h after injection in 12 of 43 patients. Two patients (patients 2 and 4) showed demarcation between tumor in the tail of the pancreas and left kidney only on late scans. In another 2 patients (patients 5 and 34), the average and maximum SUVs of the tumor increased by over 100% in the late scan, yet a confident diagnosis of insulinoma was made with early images only. Furthermore, there was no significant difference in SUVs or tumor-to-pancreas uptake ratios between dual time points for lesions visualized both on early scans and on late scans.

DISCUSSION

Several reports have provided proof that GLP-1R imaging is a sensitive tool for preoperatively localizing insulinoma in humans (10–13,26,27). Most patients were studied with exendin-4 labeled with ^{111}In (10,11,13) and ^{99m}Tc (12), and recently the use of ^{68}Ga-labeled exendin-4 PET/CT on a small number of patients with insulinoma was reported (26,27). In accordance with previous results, our prospective cohort study determined that ^{68}Ga-NOTA-exendin-4 PET/CT is sensitive for preoperative localization of insulinomas.

The sensitivity of ^{68}Ga-NOTA-exendin-4 PET/CT in localizing insulinoma is 97.7%, which is greater than that of CT (74.4%), MRI (56.0%), EUS (84.0%), and SRS (19.5%).

Pathologic studies have shown a high incidence and density of GLP-1R expression in human insulinoma (8,9), and there is an absence of the gray zone of mild to moderate receptor expression that could make in vivo assessment by PET and SPECT challenging; that is, all tumors either demonstrated high-density receptor expression or were completely negative (30). In our study, ^{68}Ga-NOTA-exendin-4 PET/CT revealed very high SUVs and tumor-to-pancreas uptake ratios in all positive scans, resulting in a confident, nonequivocal diagnosis of insulinoma. Even in 11 patients who had insulinomas smaller than 1.0 cm and were injected with no more than 55 MBq of ^{68}Ga-NOTA-exendin-4, GLP-1R PET/CT correctly localized all tumors, as confirmed by histology. Two (4.7%) of 43 patients had a confirmed diagnosis of multiple endocrine neoplasia type 1, which is consistent with previous data (31). In both patients, GLP-1R PET/CT was positive, finding all 5 lesions, whereas CT missed an 8-mm lesion. The highly radioactive kidneys may hamper the detection of tumor in the tail of the pancreas. In 2 patients, tumor could be delineated from kidney on only late scans. As the effective half-life of exendin-4 is longer in tumors than in the kidneys (11), we suggest that patients who have negative results on early scans should undergo additional imaging 2–3 h after injection.

The only false-negative result was a type G2 insulinoma that was photopenic on ^{68}Ga-NOTA-exendin-4 PET/CT, suggestive of a lack of GLP-1R expression. However, the tumor was positive on SRS. These findings corroborate with a previous conclusion that all insulinomas should be localized with the combination of GLP-1R and sstr2 imaging methods, because insulinomas always express either one or both of these receptors (30). It has been reported that malignant insulinomas express sstr2 more often than GLP-1R (73% vs. 36%) (30), yet the only patient with malignant insulinoma in our study showed high uptake in all lesions on both GLP-1R PET/CT and SRS. Concomitant expression of GLP-1R and sstr2 might be alternatively targeted for peptide receptor radionuclide therapy.

In our study, we did not observe any false-positive results with ^{68}Ga-NOTA-exendin-4 PET/CT. By contrast, a previous prospective multicenter study (with 30 recruited patients) showed a relatively low specificity of ^{111}In-DTPA-exendin-4 SPECT/CT for insulinoma (20%), because on histology it was found that there were 4 false-positive results and only 1 patient with a true-negative result (13). The discrepancy about false positivity might be explained by advantages of PET over SPECT regarding partial-volume effect and spatial resolution, as was also suggested in a recent pilot study comparing the detection rates of ^{68}Ga-DOTA-exendin-4 PET/CT and ^{111}In-DOTA-exendin-4 SPECT/CT (26).

Although not confirmed at histology, 4 patients clinically diagnosed as having nesidioblastosis showed negative results on GLP-1R PET/CT. Interestingly, a mild to moderate increase in radioactivity was noted in certain segments or the whole pancreas. A recent case report showed promising results for the diagnosis of nesidioblastosis with ^{68}Ga-DOTA-exendin-4 (32). Whether GLP-1R PET/CT is helpful in distinguishing focal from diffuse types of nesidioblastosis to aid the surgical strategy remains to be determined.

CONCLUSION

This study confirmed that ^{68}Ga-NOTA-exendin-4 PET/CT is highly sensitive for the detection of insulinomas—higher than CT, MR, EUS, and SRS. Although having a low detection rate of insulinoma with ^{99m}Tc-HYNIC-TOC SPECT/CT, SRS is clinically relevant in view of its ability to detect GLP-1R–negative insulinomas.

Supplementary Material

Refer to Web version on PubMed Central for supplementary material.

Acknowledgments

REFERENCES

1. Fidler JL, Fletcher JG, Reading CC, et al. Preoperative detection of pancreatic insulinomas on multiphasic helical CT. AJR. 2003; 181:775–780. [PubMed: 12933480]

2. McAuley G, Delaney H, Colville J, et al. Multimodality preoperative imaging of pancreatic insulinomas. Clin Radiol. 2005; 60:1039–1050. [PubMed: 16179163]

3. Sotoudehmanesh R, Hedayat A, Shirazian N, et al. Endoscopic ultrasonography (EUS) in the localization of insulinoma. Endocrine. 2007; 31:238–241. [PubMed: 17906369]

4. Rostambeigi N, Thompson GB. What should be done in an operating room when an insulinoma cannot be found? Clin Endocrinol (Oxf). 2009; 70:512–515. [PubMed: 19170712]

5. Grant CS. Insulinoma. Best Pract Res Clin Gastroenterol. 2005; 19:783–798. [PubMed: 16253900]

6. Krenning EP, Kwekkeboom DJ, Reubi JC, et al. ^{111}In-octreotide scintigraphy in oncology. Metabolism. 1992; 41:83–86. [PubMed: 1355591]

7. Krenning EP, Kwekkeboom DJ, Bakker WH, et al. Somatostatin receptor scintigraphy with [^{111}In-DTPA-D-Phe^1]- and [^{123}I-Tyr^3]-octreotide: the Rotterdam experience with more than 1000 patients. Eur J Nucl Med. 1993; 20:716–731. [PubMed: 8404961]

8. Reubi JC, Waser B. Concomitant expression of several peptide receptors in neuroendocrine tumours: molecular basis for in vivo multireceptor tumour targeting. Eur J Nucl Med Mol Imaging. 2003; 30:781–793. [PubMed: 12707737]

9. Körner M, Christ E, Wild D, Reubi JC. Glucagon-like peptide-1 receptor over-expression in cancer and its impact on clinical applications. Front Endocrinol (Lausanne). 2012; 3:158. [PubMed: 23230431]

10. Wild D, Macke H, Christ E, Gloor B, Reubi JC. Glucagon-like peptide 1-receptor scans to localize occult insulinomas. N Engl J Med. 2008; 359:766–768. [PubMed: 18703486]

11. Christ E, Wild D, Forrer F, et al. Glucagon-like peptide-1 receptor imaging for localization of insulinomas. J Clin Endocrinol Metab. 2009; 94:4398–4405. [PubMed: 19820010]

12. Sowa-Staszczak A, Pach D, Mikolajczak R, et al. Glucagon-like peptide-1 receptor imaging with [Lys^{40}(Ahx-HYNIC-^{99m}Tc/EDDA)NH$_2$]-exendin-4 for the detection of insulinoma. Eur J Nucl Med Mol Imaging. 2013; 40:524–531. [PubMed: 23224740]

13. Christ E, Wild D, Ederer S, et al. Glucagon-like peptide-1 receptor imaging for the localisation of insulinomas: a prospective multicentre imaging study. Lancet Diabetes Endocrinol. 2013; 1:115–122. [PubMed: 24622317]

14. Wild D, Wicki A, Mansi R, et al. Exendin-4-based radiopharmaceuticals for glucagonlike peptide-1 receptor PET/CT and SPECT/CT. J Nucl Med. 2010; 51:1059–1067. [PubMed: 20595511]

15. Gao H, Niu G, Yang M, et al. PET of insulinoma using ^{18}F-FBEM-EM3106B, a new GLP-1 analogue. Mol Pharm. 2011; 8:1775–1782. [PubMed: 21800885]

16. Wu Z, Todorov I, Li L, et al. In vivo imaging of transplanted islets with ^{64}Cu-DO3A-VS-Cys^{40}-exendin-4 by targeting GLP-1 receptor. Bioconjug Chem. 2011; 22:1587–1594. [PubMed: 21692471]

17. Connolly BM, Vanko A, McQuade P, et al. Ex vivo imaging of pancreatic beta cells using a radiolabeled GLP-1 receptor agonist. Mol Imaging Biol. 2012; 14:79–87. [PubMed: 21394533]

18. Kiesewetter DO, Gao H, Ma Y, et al. ^{18}F-radiolabeled analogs of exendin-4 for PET imaging of GLP-1 in insulinoma. Eur J Nucl Med Mol Imaging. 2012; 39:463–473. [PubMed: 22170321]

19. Kiesewetter DO, Guo N, Guo J, et al. Evaluation of an [^{18}F]AlF-NOTA analog of exendin-4 for imaging of GLP-1 receptor in insulinoma. Theranostics. 2012; 2:999–1009. [PubMed: 23139727]

20. Wang Y, Lim K, Normandin M, Zhao X, Cline GW, Ding YS. Synthesis and evaluation of [^{18}F]exendin-(9-39) as a potential biomarker to measure pancreatic beta-cell mass. Nucl Med Biol. 2012; 39:167–176. [PubMed: 22033026]

21. Selvaraju RK, Velikyan I, Johansson L, et al. In vivo imaging of the glucagon like peptide 1 receptor in the pancreas with ^{68}Ga-labeled DO3A-exendin-4. J Nucl Med. 2013; 54:1458–1463. [PubMed: 23761918]

22. Wu Z, Liu S, Hassink M, et al. Development and evaluation of ^{18}F-TTCO-Cys^{40}-exendin-4: a PET probe for imaging transplanted islets. J Nucl Med. 2013; 54:244–251. [PubMed: 23297075]

23. Wu H, Liang S, Liu S, Pan Y, Cheng D, Zhang Y. ^{18}F-radiolabeled GLP-1 analog exendin-4 for PET/CT imaging of insulinoma in small animals. Nucl Med Commun. 2013; 34:701–708. [PubMed: 23652208]

24. Mikkola K, Yim CB, Fagerholm V, et al. ^{64}Cu- and ^{68}Ga-labelled [Nle^{14},Lys^{40}(Ahx-NODAGA)NH$_2$]-exendin-4 for pancreatic beta cell imaging in rats. Mol Imaging Biol. 2014; 16:255–263. [PubMed: 24101374]

25. Jodal A, Lankat-Buttgereit B, Brom M, Schibli R, Behe M. A comparison of three $^{67/68}$Ga-labelled exendin-4 derivatives for beta-cell imaging on the GLP-1 receptor: the influence of the conjugation site of NODAGA as chelator. EJNMMI Res. 2014; 4:31. [PubMed: 25006548]

26. Antwi K, Fani M, Nicolas G, et al. Localization of hidden insulinomas with ^{68}Ga-DOTA-exendin-4 PET/CT: a pilot study. J Nucl Med. 2015; 56:1075–1078. [PubMed: 25999434]

27. Luo Y, Yu M, Pan Q, et al. ^{68}Ga-NOTA-exendin-4 PET/CT in detection of occult insulinoma and evaluation of physiological uptake. Eur J Nucl Med Mol Imaging. 2015; 42:531–532. [PubMed: 25398421]

28. Cryer PE, Axelrod L, Grossman AB, et al. Evaluation and management of adult hypoglycemic disorders: an Endocrine Society clinical practice guideline. J Clin Endocrinol Metab. 2009; 94:709–728. [PubMed: 19088155]

29. Doyle ME, Egan JM. Mechanisms of action of glucagon-like peptide 1 in the pancreas. Pharmacol Ther. 2007; 113:546–593. [PubMed: 17306374]

30. Wild D, Christ E, Caplin ME, et al. Glucagon-like peptide-1 versus somatostatin receptor targeting reveals 2 distinct forms of malignant insulinomas. J Nucl Med. 2011; 52:1073–1078. [PubMed: 21680696]

31. Placzkowski KA, Vella A, Thompson GB, et al. Secular trends in the presentation and management of functioning insulinoma at the Mayo Clinic, 1987-2007. J Clin Endocrinol Metab. 2009; 94:1069–1073. [PubMed: 19141587]

32. Christ E, Wild D, Antwi K, et al. Preoperative localization of adult nesidioblastosis using Ga-DOTA-exendin-4-PET/CT. Endocrine. 2015; 50:821–823. [PubMed: 26001537]
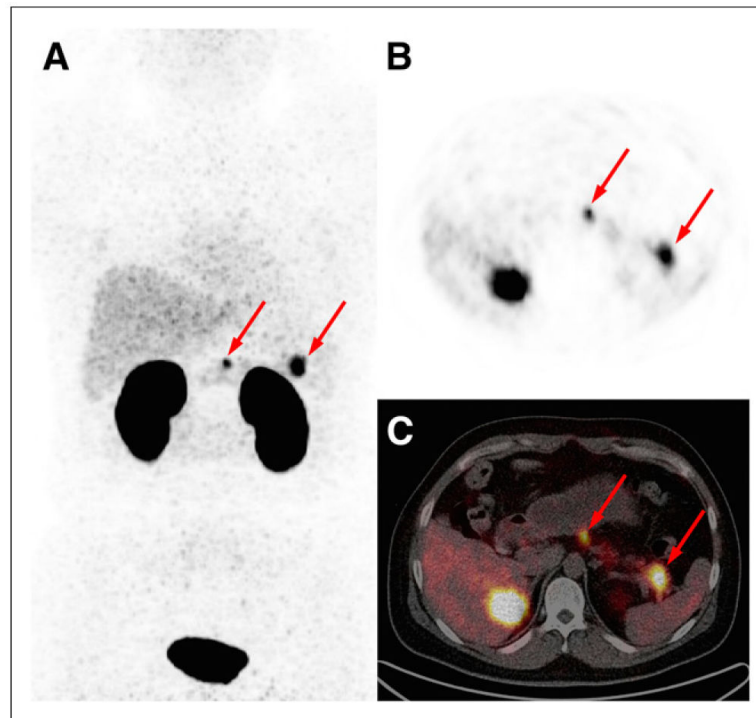
FIGURE 1.
Maximum-intensity-projection (A) and axial PET (B) and axial PET/CT (C) images
obtained from patient 33 (37-y-old 97-kg man) 40 min after injection of 18.5 MBq (7 μg)
of ^{68}Ga-NOTA-exendin-4 (4 min/bed position). Two lesions with intense focus of uptake are
seen in neck and tail of pancreas (arrows), with SUV_{max} of 10.2 and 17.3. Both lesions were
surgically removed and histologically diagnosed as insulinoma. Patient had confirmed
diagnosis of multiple endocrine neoplasia type 1.
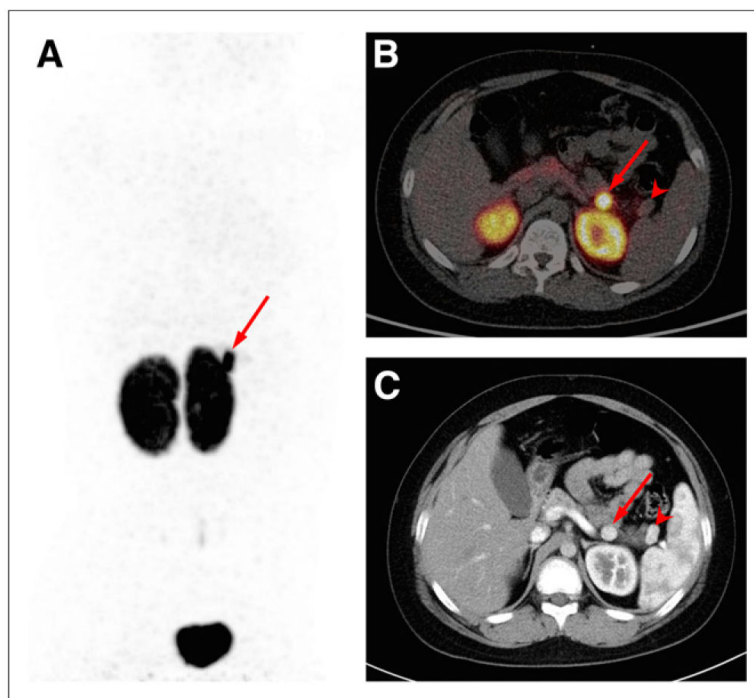
FIGURE 2.
Maximum-intensity-projection PET (A) and axial PET/CT (B) images obtained from patient 42 (10-y-old 56-kg boy) 1 h after injection of 48.1 MBq (10 μg) of ^{68}Ga-NOTA-exendin-4. Arrow shows intense focus of uptake in body of pancreas (SUV$_{max}$, 27.1), consistent with surgically removed insulinoma. Another lesion in tail of pancreas (arrowhead), possibly intrapancreatic accessory spleen, is photopenic. (C) Arterial-phase contrast-enhanced CT image from same patient. Histologically confirmed insulinoma (arrow) and intrapancreatic accessory spleen (arrowhead) show similarly intense arterial enhancement.

TABLE 1

Clinical Characteristics of the 52 Recruited Patients

Characteristic	Data
Age (y)	9–66
Sex	23 M, 29 F
Duration of symptoms	1 mo to 15 y
Spontaneous hypoglycemia present	42 patients
Fasting test result	10 patients [*]
Glucose level (mmol/L)	0.6–2.8
C-peptide level (ng/mL)	1.2–10.9
Insulin level (μIU/mL)	5.53–185.64

[*] Neuroglycopenia induced after 4–36 h.

TABLE 2

Imaging, Surgical, and Histologic Results from 43 Patients with Insulinoma

Patient no.	CT	MR	EUS	SRS	GLP-1R PET/CT	Surgery	Histology/WHO grade	Location	Size (mm)
1	FN	FN	TP	FN	TP	Enucleation	Insulinoma/G1	Head of pancreas	8
2	FN	FN	FN[*]	FN	TP	Enucleation	Insulinoma/G1	Tail of pancreas	15
3	FN	ND	TP	FN	TP	Enucleation	Insulinoma/G2	Neck of pancreas	12
4	TP	FN	TP	FN	TP	DP	Insulinoma/G1	Tail of pancreas	12
5	TP	ND	TP	FN	TP	Enucleation	Insulinoma/G1	Tail of pancreas	16
6	TP	TP	TP	TP	TP	Enucleation	Insulinoma/G2	Body of pancreas	13
7	TP	TP	ND	TP	FN	DP	Insulinoma/G2	Tail of pancreas	50
8	TP	ND	TP	TP	TP	Enucleation	Insulinoma/G1	Uncinate process	15
9	TP	FN	FN	FN	TP	Enucleation	Insulinoma/G1	Tail of pancreas	17
10	FN	ND	TP	TP	TP	Enucleation	Insulinoma/G1	Uncinate process	21
11	TP	ND	ND	FN	TP	DP	Insulinoma/G2	Tail of pancreas	20
12	TP	ND	ND	ND	TP	Enucleation[†]	insulinoma	Uncinate process	12[‡]
13	FN	FN	TP	FN	TP	Enucleation	Insulinoma/G1	Head of pancreas	15
14	FN	FN	FN	FN	TP	Enucleation	Insulinoma/G2	Tail of pancreas	24
15	+	+	ND	+	+	Liver biopsy	Insulinoma/G1	Body of pancreas, distant metastasis	NA
16	TP[§]	ND	ND	FN	TP[§]	Enucleation + DP	3 insulinomas/G2 (MEN1)	Uncinate process, neck and tail of pancreas	11, 16, 68
17	TP	FN	TP	FN	TP	Enucleation	Insulinoma/G1	Neck of pancreas	17
18	FN	ND	TP	FN	TP	Enucleation	Insulinoma/G1	Neck of pancreas	15
19	TP	FN	ND	FN	TP	Enucleation[†]	Insulinoma	Uncinate process	11[†]
20	TP	ND	FN	FN	TP	DP	Insulinoma/G2	Body of pancreas	10
21	TP	FN	ND	FN	TP	Enucleation	Insulinoma/G1	Tail of pancreas	10
22	TP	FN	ND	FN	TP	Enucleation	Insulinoma/G1	Uncinate process	10
23	TP	ND	TP	FN	TP	Enucleation	Insulinoma/G1	Head of pancreas	7
24	TP	ND	ND	FN	TP	Enucleation	Insulinoma/G1	Head of pancreas	9
25	TP	ND	TP	FN	TP	Enucleation	Insulinoma/G1	Head of pancreas	14
26	TP[*]	ND	TP	FN	TP	Enucleation	Insulinoma/G1	Body of pancreas	12
27	FN	ND	TP	FN	TP	DP	Insulinoma/G1	Body of pancreas	16
28	TP	ND	ND	FN	TP	Enucleation	Insulinoma/G2	Uncinate process	12
29	TP	ND	TP	FN	TP	Enucleation	Insulinoma/G1	Body of pancreas	10
30	TP	TP	TP	TP	TP	Enucleation	Insulinoma/G2	Uncinate process	20
31	TP	ND	ND	FN	TP	Enucleation	Insulinoma/G1	Tail of pancreas	11
32	TP	ND	ND	FN	TP	Enucleation	Insulinoma/G2	Uncinate process	14
33	FN	TP	TP	FN	TP	DP	2 insulinomas/G1 (MEN1)	Neck of pancreas	8
	TP	TP	TP	TP	TP			Tail of pancreas	25
34	TP	FN	TP	TP	TP	Enucleation	Insulinoma/G1	Uncinate process	10

Patient no.	CT	MR	EUS	SRS	GLP-1R PET/CT	Surgery	Histology/WHO grade	Location	Size (mm)
35	TP	TP	TP	ND	TP	DPRHP	Insulinoma/G2	Head of pancreas	25
36	TP	TP	ND	FN	TP	Enucleation	Insulinoma/G1	Tail of pancreas	18
37	FN	TP	ND	FN	TP	Enucleation	Insulinoma/G2	Head of pancreas	22
38	TP	TP	ND	FN	TP	Enucleation	Insulinoma/G1	Uncinate process	10
39	TP	TP	ND	FN	TP	DP	Insulinoma/G2	Tail of pancreas	8
40	FN	TP	TP	FN	TP	Enucleation	Insulinoma/G2	Neck of pancreas	15
41	FN	TP	TP	FN	TP	Enucleation	Insulinoma/G1	Uncinate process	10
42	TP*	TP*	ND	FN	TP	Enucleation†	Insulinoma	Body of pancreas	14‡
43	TP	TP	ND	FN	TP	Enucleation	Insulinoma/G1	Head of pancreas	8

*Additional false-positive lesion was detected.

†Done in other hospital.

‡Measured on CT.

§3 lesions.

FN = false-negative; TP = true-positive; DP = distal pancreatectomy; + = positive result; ND = not done; NA = not applicable; MEN1 = multiple endocrine neoplasia type 1; DPRHP = duodenum-preserving resection of head of pancreas.

TABLE 3

Comparison of GLP-1R PET/CT and Conventional Imaging in Patients with Insulinoma

Parameter	Patient-based analysis					Lesion-based analysis				
	GLP-1R PET/CT (*n* = 43)	CT (*n* = 43)	MR (*n* = 25)	EUS (*n* = 25)	SRS (*n* = 41)	GLP-1R PET/CT (*n* = 45)	CT (*n* = 45)	MR (*n* = 25)	EUS (*n* = 26)	SRS (*n* = 43)
Sensitivity	97.7%	74.4%	56.0%	84.0%	19.5%	97.8%	73.3%	56.0%	84.6%	16.3%
95% CI	87.7–99.9	58.8–86.5	34.9–75.6	63.9–95.5	8.8–34.9	88.2–99.9	58.1–85.4	34.9–75.6	65.1–95.6	6.8–30.7
P	NA	0.006	0.006	0.125	<0.001	NA	0.003	0.006	0.125	<0.001
PPV	—	—	—	—	—	100%	94.3%	93.3%	95.7%	100%
95% CI	—	—	—	—	—	92.0–100	80.8–99.3	68.1–99.8	78.1–99.9	59.0–100
P	NA	NA	NA	NA	NA	NA	0.147	0.306	0.308	NA

CI = confidence interval; NA = not applicable.

Patient 15, with multiple distant metastases, was excluded from lesion-based analysis. Positive predictive value (PPV) was not assessed in patient-based analysis because all patients were diagnosed with insulinoma in this cohort. *P* value was analyzed between GLP-1R PET/CT and each type of conventional imaging.